International Journal of Modern Physics B
Vol. 26, Nos. 27 & 28 (2012) 1243002 (17 pages)

DOI: 10.1142/S0217979212430023

QUANTUM DISCORD IN A SPIN SYSTEM WITH SYMMETRY BREAKING

BRUNO TOMASELLO[*,†,‡], DAVIDE ROSSINI[§],
ALIOSCIA HAMMA[¶] and LUIGI AMICO[*]

[*]*MATIS-INFM-CNR & Dipartimento di Fisica e Astronomia, 95123 Catania, Italy*
[†]*SEPnet and Hubbard Theory Consortium, University of Kent,*
Canterbury CT2 7NH, UK
[‡]*ISIS facility, STFC Rutherford Appleton Laboratory,*
Harwell Oxford Campus, Didcot OX11 0QX, UK
[§]*NEST, Scuola Normale Superiore & Istituto Nanoscienze-CNR,*
Piazza dei Cavalieri 7, I-56126 Pisa, Italy
[¶]*Perimeter Institute for Theoretical Physics, 31 Caroline St. N,*
Waterloo ON, N2L 2Y5, Canada
[†]*bruno.tomasello@stfc.ac.uk*

Published 15 September 2012

We analyze the *quantum discord* Q throughout the low temperature phase diagram of the quantum XY model in transverse field. We first focus on the $T = 0$ order–disorder quantum phase transition QPT both in the symmetric ground state and in the symmetry broken one. Beside it, we highlight how Q displays clear anomalies also at a noncritical value of the control parameter inside the ordered phase, where the ground state is completely factorized. We evidence how the phenomenon is in fact of collective nature and displays universal features. We also study Q at finite temperature. We show that, close to the QPT, Q exhibits quantum-classical crossover of the system with universal scaling behavior. We evidence a nontrivial pattern of thermal correlations resulting from the factorization phenomenon.

Keywords: Quantum phase transitions; quantum information; quantum correlations.

1. Introduction

Correlations provide a characterization of many-body systems.[1] In the quantum realm, beside classical correlations, nonlocal quantum correlations (like *entanglement*) play a pivotal role. Although entanglement completely describes quantum correlation for *pure* states, it is in general more subtle to characterize the pattern of correlations for *mixed* states. Indeed the quantitative interplay between classical and quantum correlations has been formulated only recently with the introduction of the *quantum discord*, operatively defining pure quantum correlations in composite systems.[2,3,5–7]

The phase diagram of spin systems displays nontrivial pattern of correlations dictated by two main features: the quantum critical point (QCP) and the factorizing point. In fact at zero temperature the system can undergo an order–disorder Quantum Phase Transition (QPT), as long as the control parameter h is tuned across a critical value h_c.[8] It is worth noting that the quantum order arises because superselection rules lead to a symmetry breaking.[4] Besides QPT, spin systems may display a further remarkable phenomenon occurring at $h = h_f$ located within the ordered symmetry broken phase, where the ground state is exactly factorized,[9–13] and therefore correlations are exclusively classical. Such factorization consists in a transition for the two-spin-entanglement[15] and is rigorously not accompanied by any change of symmetry.

In this article we analyze the quantum discord arising of the quantum XY spin system both at zero and finite temperature. In particular we consider the ground state with broken symmetry. We show that, besides the usual critical behavior at the QPT, the quantum discord displays dramatic changes also at the factorizing point, within the ordered phase (i.e., with nonvanishing spontaneous magnetization). We complete our study by detecting how the quantum critical and the factorization point affect the quantum discord at low-temperature, thus opening the way towards actual observations. The structure of this paper is as follows. In the first section an overview is given about the current notions of quantum and classical correlation in a general quantum system. In the second one we introduce a many body system suitable for our type of analysis; the Hamiltonian of the model is introduced together with few fundamental features related to its physics. In the third section we show our analysis and results at zero temperature and then once the temperature is switched on.

2. Quantum, Classical, and Total Correlations

In a bipartite system AB the total amount of correlations between A and B is given by the mutual information

$$I(A:B) \equiv S(\hat{\rho}^A) + S(\hat{\rho}^B) - S(\hat{\rho}^{AB}) , \tag{1}$$

where $S(\hat{\rho}) = -\mathrm{Tr}[\hat{\rho} \ln \hat{\rho}]$ is the von Neumann entropy. In the classical information, using the *Bayes rule*, an equivalent formulation of mutual information is:

$$J(A:B) \equiv S(A) - S(A|B) , \tag{2}$$

where the conditional entropy $S(A|B) = S(AB) - S(B)$ quantifies the ignorance on part A once a measurement on B is performed. But in the quantum realm a measurement in general perturbs the system and part of the information itself is lost. So when we consider a quantum composite system the Eq. (2) differs from Eq. (1). This *difference* allow us to estimate the relative role of quantum and classical correlations in quantum composite systems.[2,3]

Indeed if we describe a measurement on part B by a set of projectors $\{\hat{B}_k\}$, then

$$\hat{\rho}^{AB}_{(k)} = \frac{1}{p_k}(\hat{\mathbb{I}}_A \otimes \hat{B}_k)\hat{\rho}^{AB}(\hat{\mathbb{I}}_A \otimes \hat{B}_k) \tag{3}$$

is the composite state conditioned to the kth outcome with probability $p_k = \mathrm{Tr}[(\hat{\mathbb{I}}_A \otimes \hat{B}_k)\hat{\rho}^{AB}(\hat{\mathbb{I}}_A \otimes \hat{B}_k)]$. This conditioned state is the key ingredient which distinguishes between classical and quantum correlations: in fact it differs in general from the pre-measurement state $\hat{\rho}^{AB}$ as well as mutual information differs from Classical correlations. Then the amount of classical correlations C is obtained by finding the set of measurements on $\{\hat{B}_k\}$ that disturbs the least the part A, i.e., by maximizing $C = \max_{\{\hat{B}_k\}}[S(\hat{\rho}^A) - S(\hat{\rho}^{AB}|\{\hat{B}_k\})]$.[2,3,5–7] Then the difference between mutual information and Classical correlations defines the so-called *Quantum Discord*

$$Q(\hat{\rho}^{AB}) \equiv I(A:B) - C(\hat{\rho}^{AB})\,. \tag{4}$$

In the estimate of quantum correlations between subsystem of a bipartite system the Entanglement has been playing a leading role, in particular about the relevance of correlations in many body systems. However Quantum Discord differs in general from Entanglement: for example, even if they are the same for pure states, they can display a very different behavior in mixed states.

3. The XY Model in Transverse Field

We will consider here an interacting pair of spin-1/2 in the anti-ferromagnetic XY chain with transverse field h. The Hamiltonian of the model

$$\hat{\mathcal{H}} = -\sum_j \left(\frac{1+\gamma}{2}\hat{\sigma}^x_j\hat{\sigma}^x_{j+1} + \frac{1-\gamma}{2}\hat{\sigma}^y_j\hat{\sigma}^y_{j+1} + h\hat{\sigma}^z_j\right), \tag{5}$$

describes the competition between two parts: the anisotropy on the xy plane (tuned by varying $\gamma \in (0,1)$ and the coupling with external magnetic field h along the z direction. Using a set of successive transformations (Jordan-Wiegner, Bogoliubov, Fourier[20]), the Pauli matrices operators $\hat{\sigma}^\alpha_j$ $(\alpha = x, y, x)$ on sites j can be expressed in terms of operators such that the Hamiltonian takes the diagonal form $\hat{\mathcal{H}} = -\sum_k \Lambda_k \eta^\dagger_k \eta_k + \mathrm{const}$. Here the system is described as a gas of noninteracting fermions, where $\eta^\dagger_k$ (η_k) is the creation (annihilation) operator of a fermion with momentum k. Furthermore the Jordan–Wiegner transformations allows an *analytic* expression for the correlation functions $g_{\alpha\alpha}(r)$ of any two spins in the chain far r sites with each other (because of translational invariance the distance between them is all that matters).[18,19] In fact the exact solution of XY model has encouraged extensively studying on the critical phenomena it displays.[17–19] In particular, during the last decade through the analysis of quantum correlations (i.e., *Entanglement*) new insights has been made in the description of the physics of the system.[21]

3.1. *The Phase Diagram*

The phase diagram of the XY model is characterized by *two* values of the applied field h.[8–10,21] It is well-known indeed that for $\gamma \in (0,1]$ the system displays a continuum QPT for $T = 0$, $h_c = 1$, of the Ising universality class with critical indices $\nu = z = 1$, $\beta = 1/8$.[8] In fact, for strong enough external fields ($h \gg h_c$) all spins tends to be aligned along the z direction, while the opposite limit ($h \ll h_c$) give rise to a spontaneous magnetization (Z_2-symmetry broken) along a direction on the xy plane, γ dependent. Then at zero temperature on the left side $h < h_c$ of the phase diagram the system is an ordered ferromagnet and the Z_2-symmetry is broken, while on the right side $h > h_c$ the quantum fluctuations leads to the disordered phase and the system is a quantum paramagnet.

At finite temperature the physics of the whole system is affected from the QCP $h = h_c$ at zero temperature. A V-shaped diagram in the $h - T$ plane emerges, characterized by the straight lines $T = |h - h_c|$ that mark the crossover region between the so-called *Quantum Critical Region* ($T > |h - h_c|$) and the *Quasi Classical* regions surrounding it.[8]

Besides the QCP h_c there's another value of the transverse field that characterize the phase diagram of the XY model. In fact at zero temperature, given a certain anisotropy γ, there is one specific value $h_f = \sqrt{1-\gamma^2}$ where the ground state is exactly factorized[9,10]

$$|\Psi^{\gamma}_{GS}\rangle = \prod_j |\psi^{\gamma}_j\rangle \,. \tag{6}$$

At this particular value of field it seems that, even though the system is in a phase with very strong quantum correlations, there is a "critical" set of values $h_f(\gamma)$ where the state is completely classical. This strange occurrence, regarded as a paradox in the first place,[9,10] seems to be strongly connected with the reshuffling of correlations among the system. In fact, a deep analysis on the behavior of Entanglement has remarkably shed new light on the relevant physics involved on h_f.[11–13] In particular it has been shown that tuning the external field from $h < h_f$ to $h > h_f$ the entanglement pattern swaps from parallel to anti-parallel.[15] Furthermore, it has been observed that at zero temperature the bipartite entanglement has a logarithmically divergent range at h_f, together with the fact that at finite temperature there is a whole region fanning out from h_f where no pairwise entanglement survives.[16]

Then there is strong evidence, that along these critical values of field and Temperature, the behavior of Entanglement, and correlations in general, play a pivotal role in the physics involved and hence in our understanding of it. In particular it seems that the interplay of Correlations when the field is tuned across h_f is the only accessible way, so far, to tackle the puzzling physics that leads to the factorized state (6). In fact we found here that the Quantum Discord allows a fine structure of the phase diagram around h_c, and most important displays a nontrivial scaling law at the factorization field h_f.

4. Classical and Quantum Correlations in the Model

In order to compute Q_r between any two spins A and B at distance r along the chain is the key ingredients are density matrices. In fact the Eq. (4) depends both on the single site density matrices $\hat{\rho}^A$, $\hat{\rho}^B$ and on the two sites density matrix of the composite subsystem $\hat{\rho}^{AB}$. Due to the translational invariance along the chain, the single site density matrix is the same for any spin (dependent only on $m_z = \langle \sigma_z \rangle /2$), in particular

$$\hat{\rho}^A = \hat{\rho}^B = \begin{pmatrix} \frac{1}{2} + m_z & 0 \\ 0 & \frac{1}{2} - m_z \end{pmatrix} . \tag{7}$$

Then the single site von Neumann entropy for both spin A and spin B is:

$$S(\hat{\rho}^A) = S(\hat{\rho}^B) = \mathcal{S}_{\rm bin}\left(\frac{1}{2} + m_z \right) \tag{8}$$

where $\mathcal{S}_{\rm bin}(p) = -p \log p - (1-p)\log(1-p)$ is the binary Shannon entropy.

On the other hand the expression of $\hat{\rho}^{AB}$ may be cumbersome. In fact, the general 2 sites reduced density matrix for an Hamiltonian model with global phase flip symmetry has the following form[27–29]:

$$\hat{\rho}_r = \begin{pmatrix} A & a & a & F \\ a & B & C & b \\ a & C & B & b \\ F & b & b & D \end{pmatrix} \tag{9}$$

in the basis $\{|00\rangle, |01\rangle, |10\rangle, |11\rangle\}$, where $|0\rangle$ and $|1\rangle$ are eigenstates of σ^z, and we'll shortly see explicitly the matrix elements.

Because of translational invariance, this density matrix depends only on the distance r between the two spins, $\hat{\rho}^{AB} = \hat{\rho}_r$. In particular note that A and B in the matrix (9) do not denote the two spins considered, but some of the following quantities related to the correlators $g_{\alpha\beta}(r) = \langle \hat{\sigma}_j^\alpha \hat{\sigma}_{j+r}^\beta \rangle$ and $g_\alpha = \langle \sigma_\alpha \rangle = 2m_\alpha$:

$$\begin{aligned} A &= \frac{1}{4}(1 + g_z + g_{zz})\,, \\ D &= \frac{1}{4}(1 - g_z + g_{zz})\,, \\ B &= \frac{1}{4}(1 - g_{zz})\,, \\ C &= \frac{1}{4}(g_{xx} + g_{yy})\,, \\ F &= \frac{1}{4}(g_{xx} - g_{yy})\,. \end{aligned} \tag{10}$$

are the parity coefficients, while

$$
\begin{aligned}
a &= \frac{1}{4}(g_x + g_{xz})\,, \\
b &= \frac{1}{4}(g_x - g_{xz})\,,
\end{aligned}
\tag{11}
$$

explicit the contribution from the symmetry breaking.

As long as the system is in the Z_2-symmetric phase the matrix element in "low case" are null ($a = b = 0$). The symmetry breaking manifest itself in a, $b \neq 0$.[27–29] In the former case the remaining nonvanishing e entries in Eq. (9) can be evaluated analytically,[18,19] and we use a fully analytical approach to compute the Quantum Discord in the so-called *thermal ground state*.[33] In this state the system approach the ground state by lowering the temperature towards the limit of $T = 0$, but for this reason the symmetry is conserved and the state is not in the "true" degenerate *ground state*. In the latter one the Z_2-symmetry is lost and beside the spontaneous magnetization m_x, also the nontrivial $g_{xz}(r)$ appears.[30] In this case we analyze the real ground state by means of *numerical* methods, i.e., Density Matrix Renormalization Group (DMRG) for finite systems with open boundaries.[31] Once we have access to the density matrices through the correlation function, we need to compute the explicit form of the mutual information and the classical correlation in order to "distill" the amount of pure quantum correlations [i.e., Quantum Discord, Eq. (4)]. Here we follow the notation used in Ref. 33. Since the reduced density matrix of the single spin is the same for any site, we have already shown in Eq. (8) that $S(\hat{\rho}^A) = S(\hat{\rho}^B)$. Hence the mutual information is:

$$
I(\hat{\rho}_r^{AB}) = 2S(\hat{\rho}^A) - \sum_{\nu=0}^{3} \lambda_\nu \log \lambda_\nu
\tag{12}
$$

where $\lambda_\nu(r)$ are eigenvalues of $\hat{\rho}_r^{AB}$, that in terms of correlation functions $g_{\alpha\alpha}(r) = \langle \hat{\sigma}_j^\alpha \hat{\sigma}^\alpha j + r\rangle$ and $g_z = 2m_z$ are[33]:

$$
\begin{aligned}
\lambda_0 &= \frac{1}{4}\Big(1 + g_{zz} + \sqrt{g_z^2 + (g_{xx} - g_{yy})^2}\Big) \\
\lambda_1 &= \frac{1}{4}\Big(1 + g_{zz} - \sqrt{g_z^2 + (g_{xx} - g_{yy})^2}\Big) \\
\lambda_2 &= \frac{1}{4}\big(1 - g_{zz} + (g_{xx} + g_{yy})\big) \\
\lambda_2 &= \frac{1}{4}\big(1 - g_{zz} - (g_{xx} + g_{yy})\big)\,.
\end{aligned}
\tag{13}
$$

Once the mutual information is known in terms of the correlation functions [Eq. (12)] we need to find the explicit form for the classical correlations in the XY model, in order to compute pure quantum correlations, as stated in Eq. (4). Following a procedure similar to Refs. 32–34, we use a set of projectors $\{\hat{B}_k\}$ as local measurements on the spin B. In particular, working on the computational basis $\{|0\rangle, |1\rangle\}$ in the Hilbert space $\mathcal{H}_B^2$ associated to the spin B, our general set of projectors is:

$$\{\hat{B}_k = V\hat{\Pi}_k V^\dagger\}, \quad k = 0, 1 \tag{14}$$

where $\hat{\Pi}_k = |k\rangle\langle k|$ related to the basis vectors and $V \in U(2)$ gives the generalization to any type of projector on B. As suggested in Ref. 33, it is useful to parametrize V as follows:

$$V = \begin{pmatrix} \cos\dfrac{\theta}{2} & \sin\dfrac{\theta}{2}e^{-i\phi} \\ \sin\dfrac{\theta}{2}e^{i\phi} & -\cos\dfrac{\theta}{2} \end{pmatrix} \tag{15}$$

where $\theta \in [0, \pi]$ and $\phi \in [0, 2\pi]$ are respectively the azimuthal and polar axes of a qubit over the *Bloch sphere* in $\mathcal{H}_B^2$. After a measurement has been performed on B the reduced density matrix $\hat{\rho}^{AB}_{\{\hat{B}_k\}}$ will be in one of the following states:

$$\begin{aligned} \hat{\rho}_0^{AB} &= \frac{1}{2}\left(\hat{\mathbb{I}}_A + \sum_{\alpha=1}^{3} q_{0\alpha}\hat{\sigma}_A^\alpha\right) \otimes (V\hat{\Pi}_0 V^\dagger)_B\,, \\ \hat{\rho}_1^{AB} &= \frac{1}{2}\left(\hat{\mathbb{I}}_A + \sum_{\alpha=1}^{3} q_{1\alpha}\hat{\sigma}_A^\alpha\right) \otimes (V\hat{\Pi}_1 V^\dagger)_B\,. \end{aligned} \tag{16}$$

This expression for the reduced density matrices gives the explicit dependence of the system A respect to the projective measurement performed on the spin B. Indeed the coefficient $q_{k\alpha} = q_{k\alpha}(\theta, \phi)$ in the expansion depend on the projectors used to perform the measure on B (see Ref. 33 for the explicit form).

We remind here the explicit form for the classical correlations[2,3,5–7]

$$C = \max_{\{\hat{B}_k\}}[S(\hat{\rho}^A) - S(\hat{\rho}^{AB}|\{\hat{B}_k\})]\,. \tag{17}$$

Maximizing over all possible $\hat{B}_k$ is equivalent to find for those values (θ, ϕ) that *disturb* the least the spin A when we make a measure on B. We found $(\theta = \pi/2, \phi = 0)$, in agree with Refs. 33 and 35. And following their same method to evaluate $S(\hat{\rho}^{AB}|\{\hat{B}_k\})$ we found a simple expression for classical correlations

$$C_r = H_{\text{bin}}(p_1) - H_{\text{bin}}(p_2)\,, \tag{18}$$

where $H_{\text{bin}}(p)$ is the Shannon entropy and

$$\begin{aligned} p_1 &= \frac{1}{2} + m_z \\ p_2 &= \frac{1}{2} + \sqrt{g_{xx}^2/4 + m_z^2}\,. \end{aligned} \tag{19}$$

So by the difference of the mutual information (12) and the latter expression for the classical correlations (18) we get the simplified expression for the quantum discord between any two spins in the XY chain in transverse field

$$Q(\hat{\rho}_r) = H_{\mathrm{bin}}(p_1) + H_{\mathrm{bin}}(p_2) - \sum_{\nu=0}^{4} \lambda_\nu \log \lambda_\nu \,. \tag{20}$$

5. Analysis of Quantum Discord at $T = 0$

In this section, we show our analysis of quantum correlations both in the thermal ground state and in the symmetry broken one. In particular we remark differences and similarities between them, and highlight the interesting features occurring at the QCP $h_c = 1$ and at the factorizing field h_f (if not specified $\gamma = 0.7$ in every picture).

We start by showing the behavior of quantum discord at zero temperature, over a wide range of external field h centered around the critical value h_c where the QPT occurs. In Fig. 1 we compare, for both the XY model ($\gamma = 0.7$ for example) and the Ising one (inset where $\gamma = 1$), the numerical results we got from DMRG

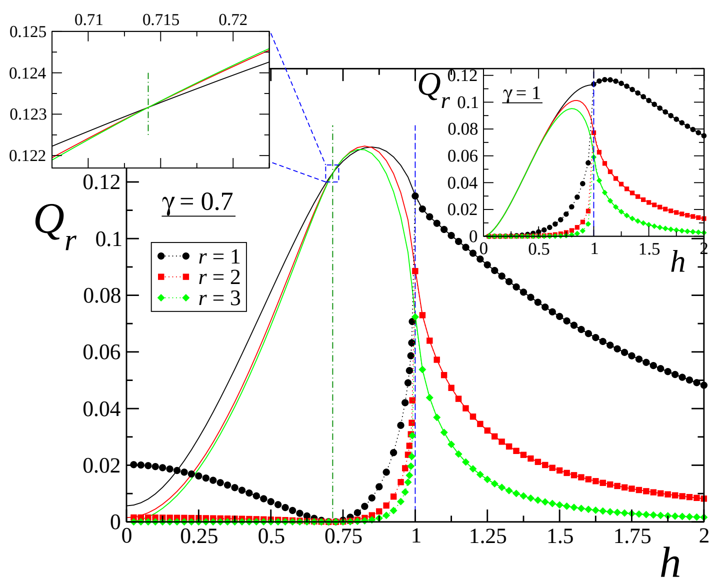

Fig. 1. Quantum discord $Q_r(h)$ between two spins at distance r in the XY model at $\gamma = 0.7$ (main plot and left inset) and $\gamma = 1$ (right inset), as a function of the field h. Continuous lines are for the thermal ground state, while symbols denote the symmetry-broken state obtained by adding a small symmetry-breaking longitudinal field $h_x = 10^{-6}$ and it was computed with DMRG in a chain of $L = 400$ spins; simulations were performed by keeping $m = 500$ states and evaluating correlators at the center of the open-bounded chain. For $\gamma = 0.7$ and at $h_f \simeq 0.714$, in the symmetric state all the curves for different values of r intersect, while after breaking the symmetry Q_r is rigorously zero. At the critical point Q_r is nonanalytic, thus signaling the QPT. In the paramagnetic phase, there is no symmetry breaking to affect Q_r.

computation of Q_r on the true ground state respect to the analytical values of the thermal ground state. There is strong evidence that in the disordered phase, $h > h_c$, no difference occurs between the two state, while in the opposite regime $h < h_c$ two different pattern comes out. In fact in the latter case, the order in the system is really achieved only in the case where the symmetry of the system is lost. We achieve this condition using a staggered field in the DMRG computation that leads to the symmetry breaking and gives out the true ground state where quantum correlations are very small as long as $h < h_c$. In particular it is remarkable that they start to increase once the field is tuned immediately upper the factorizing field, where all quantum correlations must vanish, to reach a cuspid-like maximum at the QCP. On the other hand, the quantum discord on the thermal ground state (solid lines in Fig. 1) is a smooth function respect to the field. In general it depends on the distance r between the two spins, but at the factorizing point it gets the same value for any length scale.[36]

To go deeper in the analysis let us focus on $h_c = 1$ in the first place. The QPT is in general marked by a divergent derivative of the quantum discord, with respect to the field. In particular such divergence is present for any γ in the symmetry broken state, while on the thermal ground state it holds as long as $\gamma < 1$ (see Fig. 2); for $\gamma = 1$, $\partial_h Q_r$ is finite at h_c although the $\partial_h^2 Q_r$ diverges.[33] This divergence suggests that a scaling analysis at the QCP is feasible. In particular in Fig. 3 we show the finite size scaling $\partial_h Q_{r=1}$ for the symmetry-broken ground state in proximity of h_c. We found that $z = \nu = 1$, thus meaning that the transition is in the Ising universality class.

Turning now into the factorizing field we underline that, for the thermal ground state, it is the only value where the curves with different r, intersect with each other

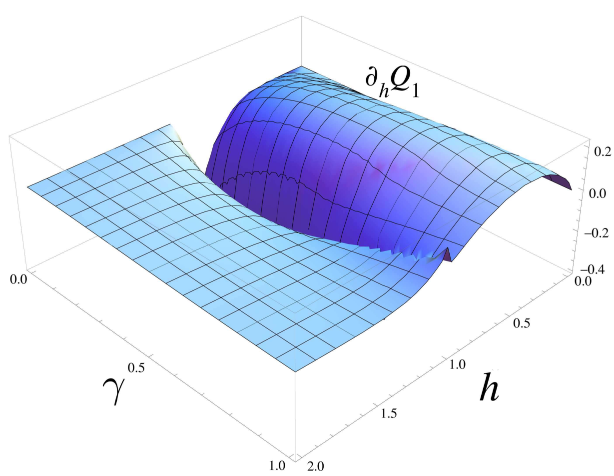

Fig. 2. Behavior of $\partial_h Q_r$ in the thermal ground state, with respect to the field for any type of anisotropy γ. Focusing at the QCP ($h = 1$), note that for $\gamma < 1$ it is divergent, while it remains finite for $\gamma = 1$.

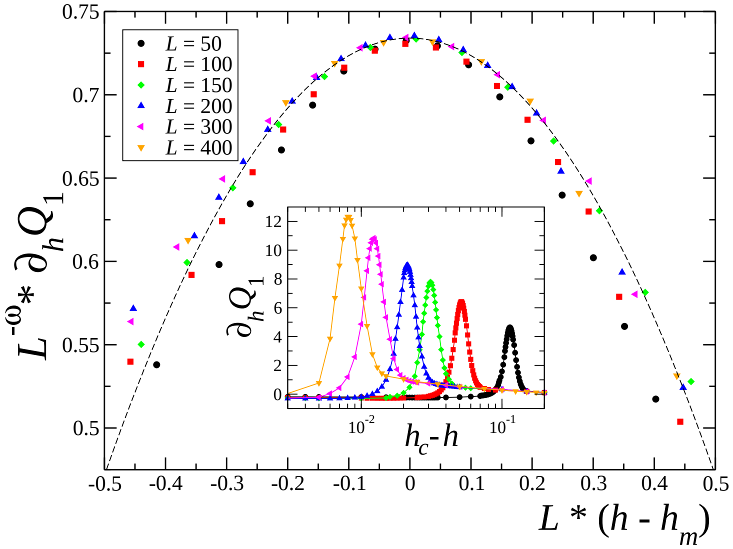

Fig. 3. Finite-size scaling of $\partial_h Q_1$ for the symmetry-broken state in proximity of the critical point h_c. Displayed data are for $\gamma = 0.7$. The first derivative of the quantum discord is a function of $L^{-\nu}(h - h_m)$ only, and satisfies the scaling ansatz $\partial_h Q_1 \sim L^{\omega} \times F[L^{-\nu}(h - h_m)]$, where h_m is the renormalized critical point at finite size L and $\omega = 0.472$. We found a universal behavior $h_c - h_m \sim L^{-1.28\pm0.03}$ with respect to γ. Inset: raw data of $\partial_h Q_1$ as a function of the transverse field.

(see up-left inset in Fig. 1).[36] Beside this, in the broken symmetry state, not only we found that all curves vanish in h_f, but we numerically estimated the following particular dependence of Q_r close to it:

$$Q_r \sim (h - h_f)^2 \times \left(\frac{1-\gamma}{1+\gamma}\right)^r . \tag{21}$$

Such behavior is consistent with the expression of correlation functions close to the factorizing line obtained in Ref. 14, and here appears to incorporate the effect arising from the nonvanishing spontaneous magnetization. Most remarkably, we found a rather peculiar dependence of Q_r on the system size, converging to the asymptotic value $Q_r^{(L\to\infty)}$ with an exponential scaling behavior (see Fig. 4).

6. Quantum Discord at Finite Temperature

Even if both the QCP h_c and the factorizing field h_f are defined at $T = 0$, they influence the whole physics of the system once the temperature is switched on. Close to h_c, the physics is dictated by the interplay between thermal and quantum fluctuations of the order parameter. As we stated before the cross-over temperature $T_{\rm cross} = |h - h_c|^z$ fixes the energy scale.[8] For $T \ll T_{\rm cross}$ the system is described by a quasi-classical theory, while inside the "quantum critical region" ($T \gg T_{\rm cross}$), it's impossible to distinguish between quantum and thermal effects. Here the critical property arising from the QCP at $T = 0$ are highly dominating the dynamics

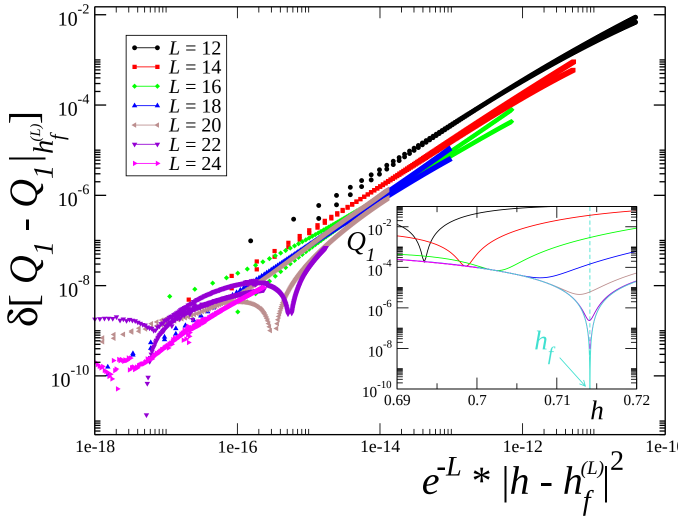

Fig. 4. Scaling of Q_1 close to the factorizing field, for $\gamma = 0.7$: we found an exponential convergence to the thermodynamic limit, with a universal behavior according to $e^{-\alpha L}(h - h_f^{(L)})$, $\alpha \approx 1$ [$h_f^{(L)}$ denotes the effective factorizing field at size L, while $\delta(Q_1) \equiv Q_1^{(L)} - Q_1^{(L\to\infty)}$]. Due to the extremely fast convergence to the asymptotic value, already at $L \sim 20$ differences with the thermodynamic limit are comparable with DMRG accuracy. Inset: raw data of Q_1 as a function of h. The cyan line is for $L = 30$ so that, up to numerical precision, the system behaves at the thermodynamic limit.

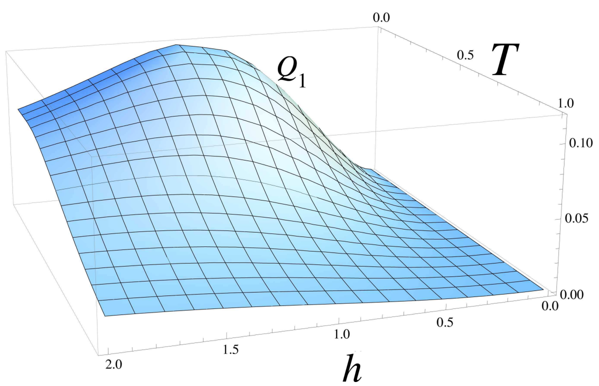

Fig. 5. Quantum discord in the thermal state of the Ising model with $\gamma = 1$, as a smooth function of temperature T and of the external field h.

of the system, and we would aspect that quantum correlations show some particular pattern as well as they do at h_c. In fact close to h_f and at small T, the bipartite entanglement remains vanishing in a finite nonlinear cone in the $h - T$ plane.[16,21] Thermal states, though, are not separable, and entanglement is present in a multipartite form.[26] In this regime the bipartite entanglement results to be nonmonotonous, and a reentrant swap between parallel and antiparallel entangle-

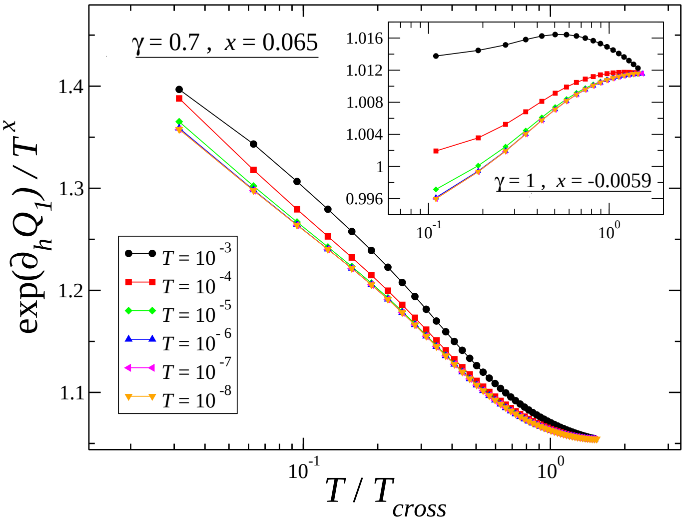

Fig. 6. Finite-temperature scaling of the quantum discord for the thermal state close to the critical point. The logarithmic scaling is verified: along the critical line we found $\partial_h Q_1|_{h_c} \sim x\ln(T) + k$, with $x = 0.065$ for $\gamma = 0.7$. The scaling function F shows a data collapse close to the critical point. Inset: same analysis for the Ising case ($\gamma = 1$); we found an analogous scaling behavior with $x = -0.0059$.

ment is observed.[16] At finite temperature, the Z_2-Symmetry is preserved all over the values of h (there is no longer a symmetry broken phase). This means that if the system lies in the ground state at $T = 0$ (symbols lines in Fig. 1), once the temperature is switched on we get a jump of Q_r all along the phase $h < h_c$. After that it behaves as a smooth function decaying with temperature (Fig. 5). Such discontinuity is also observed in the entanglement, even if in that case it is much less pronounced and occurs only for $h < h_f$.[27–29] We now analyze how criticality and factorization modify the fabric of pure quantum correlations in the $h - T$ plane.

We start by focusing on the finite-temperature scaling of the quantum discord close to the critical point h_c. In the first place we verified the logarithmic scaling $\partial_h Q_r|_{h_c} \sim x\ln(T) + k$ along the critical line, $h = 1$ in the $h - T$ plane (see Fig. 9), where the value of x depends on the degree of anisotropy γ. Once x is given (for example we found $x = 0.065$ for $r = 1$, $\gamma = 0.7$, Fig. 6), by properly tuning the ratio T/T_{cross}, where $T_{\text{cross}} \equiv |h - h_c|$, we verified the scaling ansatz

$$\partial_h Q_r = T^x F\left(\frac{T}{T_{\text{cross}}}\right). \tag{22}$$

In particular in Fig. 6 we show how different curves, related to different values of T/T_{cross}, collapse when approaching the critical point. Remarkably in the Ising case (inset) the scaling is verified as well, even if the derivative $\partial_h Q_1$ is finite at h_c. To explore the behavior of correlations along the $h - T$ plane we studied how the quantum discord varies on the phase diagram just above the QCP. In the first place

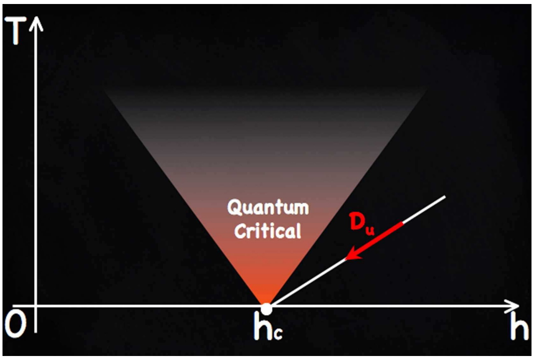

Fig. 7. Schematic representation for the directional derivative on the phase diagram. It allows to study how quantities vary along straight lines coming out from the critical point with slope $\mathbf{u} \equiv (\cos\alpha, \sin\alpha)$.

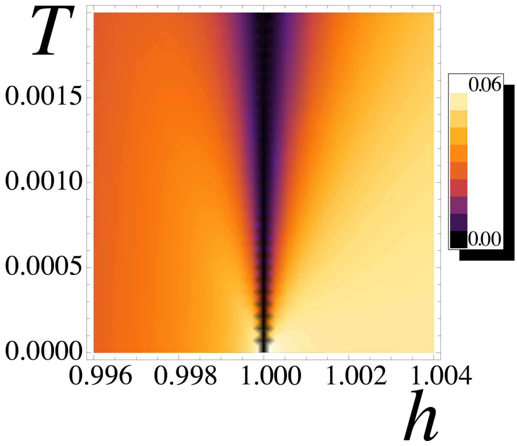

Fig. 8. Density plot in the $h - T$ plane of $D_{\mathbf{u}}Q_1$ close to h_c; The vertical line starting from the QCP shows that Q_1 tends to be constant inside the quantum critical region.

we analyze how the derivative respect to field behaves along the directions fanning out from h_c. In Fig. 7 we sketch a cartoon to describe the directional derivative $D_{\mathbf{u}}Q = |\partial_T Q \sin\alpha + \partial_a Q \cos\alpha|$ we used to describe how Q_1 varies close to the QCP. From the pattern of $D_{\mathbf{u}}Q_1$ at low temperature (Fig. 8) we see how the presence of the QPT charaterizes the whole phase diagram. The black vertical line starting from the QCP highlights the fact that the quantum discord remains constant along the critical line $h = 1$: in a sense, close to such region $h \approx 1$, quantum correlations are particularly "rigid". This explains their robustness up to finite temperatures, particularly along slopes within the quantum critical region. On the other hand, out of the quantum critical region, the variation of Q_1 is drastically increased. We also point out the peculiar asymmetric behavior between the two semiclassical regions (in the ordered phases $D_{\mathbf{u}}Q_1$ is generally higher than in the paramagnetic phase).

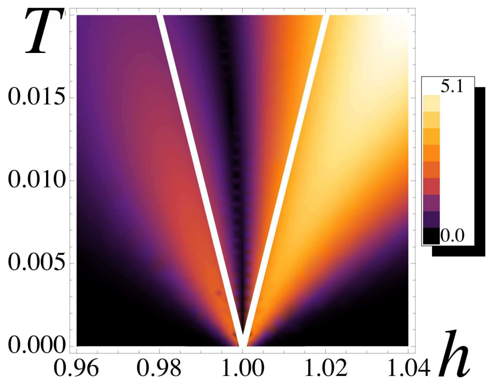

Fig. 9. Density plot in the $h-T$ plane of $\partial_T[Q_1/C_1]$ close to h_c; along the critical line the ratio Q_1/C_1 is constant with respect to the temperature. The solid straight line ($T = |h - h_c|$) marks the boundary of the quantum critical region.

Furthermore, to make a more accurate analysis we look at the interplay between quantum discord and classical correlations. In particular we analyze how this ratio Q_1/C_1 varies with the temperature, exploiting the respective sensitivity to thermal fluctuations arising at finite temperature. Accordingly with the phase diagram related to the QPT, a V shaped pattern comes out (see Fig. 9). In particular along the critical line, inside the quantum critical region, we found $\partial_T[Q_1/C_1] = 0$. Then apparently the ratio between correlations is constant even though the temperature is switched on, as long as the field is tuned at the critical value h_c. Beside this, the whole crossover region from a phase to another is marked as the highest variation in the nature of correlations in the system. In conclusion we analyze how the factorizing field affects the physics of the system at nonzero temperature. As we emphasized before, the Z_2-symmetry is preserved on the thermal state. In par-

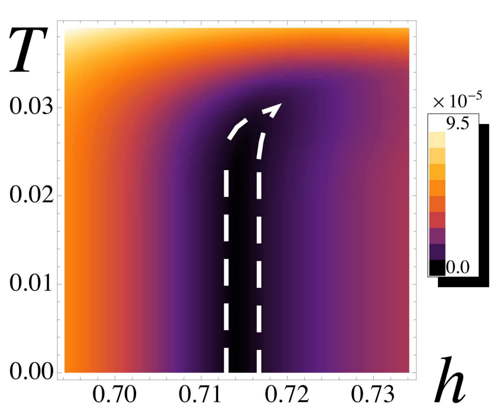

Fig. 10. Average quantum discord displacement: $\overline{\Delta Q_r} = 2\sum_{i,j=1}^{m} |Q_{r_i} - Q_{r_j}|/m(m-1)$ for $m = 5$ fanning out from the factorizing point $h_f \sim 0.714$, where all correlations coincide at any length scale r, as evidenced in the left inset of Fig. 1. Here $\gamma = 0.7$.

ticular we highlighted also that for the thermal ground state, the factorizing field was the unique value where the quantum discord is the same at any length scale r. Here we found that indeed this feature is present even after the temperature is switched on. In fact in Fig. 10 we propose $\overline{\Delta Q_r} = 2\sum_{i,j=1}^{m} |Q_{r_i} - Q_{r_j}|/m(m-1)$ as a measure of the robustness of this characteristic at nonzero temperature. We consider different distances between the couple of spin A and B, and we take the average of the difference between the respective quantum discord. There is strong evidence in Fig. 10 that for a finite range of temperature this difference is still zero (i.e., the quantum discord for different r is still the same only at h_f).

Here we emphasize that the robustness and sensitivity of the quantum discord to nonzero temperature, encourage the implementation of suitable experiments that could give good feedback of our analysis.

7. Discussions

We studied pure quantum correlations quantified by the quantum discord Q_r in the quantum phases involved in a symmetry-breaking QPT. In the ordered phase, although Q_r results relatively small in the symmetry broken state as compared to the thermal ground state, it underlies key features in driving both the order–disorder transition across the QPT at h_c, and the correlation transition across the factorizing field h_f. The critical point is characterized by a nonanalyticity of Q_r found in the Ising universality class. Close to h_f, Q_r displays uniquely nontrivial properties: in the thermal ground state quantum correlations are identical at all scales; for the symmetry broken state the factorization can be interpreted as a collective reshuffling of quantum correlations. We point out that h_f marks the transition between two "phases" characterized by a different pattern of entanglement.[15,16] Accordingly our data provide evidence that such a *correlation transition* phenomenon is of collective nature, governed by an exponential scaling law. We observe that the scaling close to h_f cannot be algebraic because the correlation functions decay exponentially in the gapped phases. We notice however that, due to the peculiar phenomenology of the factorizing phenomenon, it can be specific for scaling beyond the generic exponential behavior that is observed in gapped phases. For finite L different ground states for the two parity sectors intersect.[22,23] The ground state energy density is diverging *for all* L (such divergence, though, vanishes in the thermodynamic limit). Indeed we found that the factorization occurs without any violation of adiabatic continuity. Accordingly, the ground state fidelity $\mathcal{F}(h)$, which can detect both symmetry breaking and nonsymmetry breaking QPT, is a smooth function at h_f.[40] We remark that this can occur without closing a gap and changing the symmetry of the system, as a signature of the fact that quantum phases and entanglement are more subtle than what the symmetry-breaking paradigm says. Such a behavior is particularly relevant in the context of QPTs involving topologically ordered phases where a QPT consists in the change of the global pattern of entanglement, instead of symmetry.[37–39]

We analyze the phase diagram at low T. A discontinuity of Q_r with T is evidenced in the whole ordered phase $h < h_c$. We proved that Q_r displays universal features, identifying the quantum critical region, as that one where the quantum discord (relatively to classical correlation) is frozen out to the $T = 0$ value. In particular we notice that in each phase the ratio between correlations is stable respect to the temperature, while the highest variation are in particular in the crossover region on the right of h_c, where the system is running out of the critical region into the quasi-classical one just above the disordered phase of the paramagnet. This aspect shows that this type of quantum correlations allows a fine structure of the phase diagram according to the behavior of the gap $\Delta \lesseqgtr 0$ in the low temperature limit $T \ll |\Delta|$, that takes into account that the mechanism leading to the two corresponding semiclassical regimes driven from quantum ($\Delta > 0$) or thermal ($\Delta < 0$) fluctuations.[8]

We have found that a nontrivial pattern of quantum correlations fans out from the factorization of the ground state as well.

Acknowledgments

We thank A. De Pasquale, R. Fazio, S. Montangero, D. Patané, M. Zannetti, J. Quintanilla for useful discussions. The DMRG code released within the PwP project (www.dmrg.it) has been used. Research at Perimeter Institute for Theoretical Physics is supported in part by the Government of Canada through NSERC and by the Province of Ontario through MRI. DR acknowledges support from EU through the project SOLID.

References

1. X.-G. Wen, *Quantum Field Theory of Many-Body Systems* (Oxford University Press, USA, 2004).
2. L. Henderson and V. Vedral, *J. Phys. A: Math. Gen.* **34**, 6899 (2001).
3. H. Ollivier and W. H. Zurek, *Phys. Rev. Lett.* **88**, 017901 (2002).
4. S. Coleman, Secret symmetry: An introduction to spontaneous symmetry breakdown and gauge fields, in *Laws of Hadronic Matter*, ed. A. Zichichi (Academic Press, New York, 1975).
5. V. Vedral, *Phys. Rev. Lett.* **90**, 050401 (2003).
6. D. Borivoce, V. Vedral and C. Bruckner, *Phys. Rev. Lett.* **105**, 190502 (2010).
7. A. Auyuanet and L. Davidovic, *Phys. Rev. A* **82**, 032112 (2010).
8. S. Sachdev, *Quantum Phase Transitions* (Cambridge University Press, Cambridge, 2001).
9. J. Kurmann, H. Thomas and G. Muller, *Physica A* **112**, 235 (1982).
10. T. Roscilde *et al.*, *Phys. Rev. Lett.* **94**, 147208 (2005).
11. S. M. Giampaolo *et al.*, *Phys. Rev. Lett.* **100**, 197201 (2008).
12. S. M. Giampaolo *et al.*, *Phys. Rev. B* **79**, 224434 (2009).
13. S. M. Giampaolo *et al.*, *Phys. Rev. Lett.* **104**, 207202 (2010).
14. F. Baroni *et al.*, *J. Phys. A: Math. Theor.* **40**, 9845 (2007).
15. A. Fubini *et al.*, *Eur. Phys. J. D* **38**, 563 (2006).
16. L. Amico *et al.*, *Phys. Rev. A* **74**, 022322 (2006).

17. P. Pfeuty, *Ann. Phys.* **57**, 79 (1970).
18. E. Barouch and B. M. McCoy, *Phys. Rev. A* **2**, 1075 (1970).
19. E. Barouch and B. M. McCoy, *Phys. Rev. A* **3**, 786 (1971).
20. E. Lieb, T. Schultz and D. Mattis, *Ann. Phys.* **16**, 407 (1961).
21. L. Amico *et al.*, *Rev. Mod. Phys.* **80**, 517 (2008).
22. G. Giorgi, *Phys. Rev. B* **79**, 060405(R) (2009).
23. A. De Pasquale and P. Facchi, *Phys. Rev. A* **80**, 032102 (2009).
24. M. Continentino, *Quantum Scaling in Many Body Systems* (World Scientific, Singapore, 2001).
25. F. Franchini *et al.*, *J. Phys. A: Math. Theor.* **40**, 8467 (2007).
26. G. Toth, private communication.
27. O. F. Syljuåsen, *Phys. Rev. A* **68**, 060301(R) (2003).
28. A. Osterloh *et al.*, *Phys. Rev. Lett.* **97**, 257201 (2006).
29. T. R. de Oliveira *et al.*, *Phys. Rev. A* **77**, 032325 (2008).
30. J. D. Johnson and B. M. McCoy, *Phys. Rev. A* **4**, 2314 (1971).
31. U. Schöllwock, *Rev. Mod. Phys.* **77**, 259 (2005).
32. R. Dillenschneider, *Phys. Rev. B* **78**, 224413 (2008).
33. M. S. Sarandy, *Phys. Rev. A* **80**, 022108 (2009).
34. S. Luo, *Phys. Rev. A* **77**, 042303 (2008).
35. J. Maziero *et al.*, *Phys. Rev. A* **82**, 012106 (2010).
36. L. Ciliberti, R. Rossignoli and N. Canosa, *Phys. Rev. A* **82**, 042316 (2010).
37. A. Hamma *et al.*, *Phys. Rev. A* **71**, 022315 (2005).
38. A. Kitaev and J. Preskill, *Phys. Rev. Lett.* **96**, 110404 (2006).
39. M. Levin and X.-G. Wen, *Phys. Rev. Lett.* **96**, 110405 (2006).
40. D. Abasto, A. Hamma and P. Zanardi, *Phys. Rev. A* **78**, 010301(R) (2008).
41. X. Chen, Z.-C. Gu and X.-G. Wen, *Phys. Rev. B* **82**, 155138 (2010).